Plant Communications
Research article

CellPress
Partner Journal

ABA signaling prevents phosphodegradation of the SR45 splicing factor to alleviate inhibition of early seedling development in *Arabidopsis*

Rui Albuquerque-Martins[1,2], Dóra Szakonyi[1], James Rowe[2], Alexander M. Jones[2,*] and Paula Duque[1,*]

[1]Instituto Gulbenkian de Ciência, 2780-156 Oeiras, Portugal

[2]Sainsbury Laboratory, University of Cambridge, Cambridge B2 1LR, UK

***Correspondence: Alexander M. Jones (amj53@cam.ac.uk), Paula Duque (duquep@igc.gulbenkian.pt)**

https://doi.org/10.1016/j.xplc.2022.100495

ABSTRACT

Serine/arginine-rich (SR) proteins are conserved splicing regulators that play important roles in plant stress responses, namely those mediated by the abscisic acid (ABA) hormone. The *Arabidopsis thaliana* SR-like protein SR45 is a described negative regulator of the ABA pathway during early seedling development. How the inhibition of growth by ABA signaling is counteracted to maintain plant development under stress conditions remains largely unknown. Here, we show that *SR45* overexpression reduces *Arabidopsis* sensitivity to ABA during early seedling development. Biochemical and confocal microscopy analyses of transgenic plants expressing fluorescently tagged SR45 revealed that exposure to ABA dephosphorylates the protein at multiple amino acid residues and leads to its accumulation, due to SR45 stabilization via reduced ubiquitination and proteasomal degradation. Using phosphomutant and phosphomimetic transgenic *Arabidopsis* lines, we demonstrate the functional relevance of ABA-mediated dephosphorylation of a single SR45 residue, T264, in antagonizing SR45 ubiquitination and degradation to promote its function as a repressor of seedling ABA sensitivity. Our results reveal a mechanism that negatively autoregulates ABA signaling and allows early plant growth under stress via posttranslational control of the SR45 splicing factor.

Key words: abscisic acid, alternative splicing, *Arabidopsis thaliana*, protein phosphorylation, SR proteins

Albuquerque-Martins R., Szakonyi D., Rowe J., Jones A.M., and Duque P. (2023). ABA signaling prevents phosphodegradation of the SR45 splicing factor to alleviate inhibition of early seedling development in *Arabidopsis*. Plant Comm. **4**, 100495.

INTRODUCTION

Serine/arginine-rich (SR) proteins are members of a highly conserved family of RNA-binding factors that play important roles in mRNA splicing. These accessory spliceosomal proteins bind to *cis*-regulatory sequences in the precursor-mRNA, promoting early spliceosome assembly and influencing splice site selection. SR proteins are thus crucial for alternative splicing, a posttranscriptional mechanism that generates multiple transcripts from the same gene and has key biological relevance in eukaryotes, namely in developmental programs and stress response. Structurally, SR proteins present one or two N-terminal RNA recognition motifs, responsible for binding transcripts, and an arginine/serine-rich (RS) protein–protein interaction domain at the C terminus that recruits core spliceosome components to splice sites. The RS domain is subjected to extensive reversible phosphorylation (reviewed in Duque, 2011), which, in animal systems, is known to be required for spliceosome assembly and has also been linked to mRNA export from the nucleus (Huang et al., 2004; Sanford et al., 2005) or to switching functions from splicing activator to repressor (Shi and Manley, 2007; Feng et al., 2008). In plant systems, SR proteins are increasingly implicated in abiotic stress responses mediated by the abscisic acid (ABA) hormone (Carvalho et al., 2010; Chen et al., 2013; Xing et al., 2015; Albaqami et al., 2019; Laloum et al., 2021).

The phytohormone ABA coordinates several developmental processes, such as seed dormancy, embryo maturation, seedling growth, and greening, but it is also pivotal in the response to environmental challenges. Sensing of osmotic or oxidative stress by

Published by the Plant Communications Shanghai Editorial Office in association with Cell Press, an imprint of Elsevier Inc., on behalf of CSPB and CEMPS, CAS.

plant cells leads to a massive increase in the levels of ABA, which is recognized by the PYR/PYL/RCAR (PYRABACTIN RESISTANCE/PYRABACTIN RESISTANCE-LIKE/REGULATORY COMPONENT OF ABA RECEPTORS) intracellular soluble receptors. Hormone–receptor binding facilitates the formation of a protein complex with PP2C (PROTEIN PHOSPHATASE 2C) phosphatases, preventing the latter from inhibiting core ABA signaling protein kinases named SnRK2s (SUCROSE NON-FERMENTING 1-RELATED PROTEIN KINASE 2). In the absence of PP2Cs, SnRK2s are activated by phosphorylation via the B-Raf-like protein MAPKKKs and can then phosphorylate specific transcription factors, such as bZIPs (BASIC LEUCINE ZIPPER), to induce the expression of stress-responsive genes (reviewed in Finkelstein, 2013; Sah et al., 2016; Fàbregas et al., 2020).

Phosphorylation-triggered protein degradation is an important strategy common to animal and plant systems (reviewed in Filipčík et al., 2017; Vu et al., 2018; Bhaskara et al., 2019). In plants, it is crucial for the regulation not only of light signaling (Al-Sady et al., 2006; Shen et al., 2007; Yue et al., 2016) but also of several important players in the ABA pathway (Liu and Stone, 2010; Li et al., 2016, 2018; Chen et al., 2018; Mizoi et al., 2019). The ubiquitin–proteasome system is a highly regulated mechanism for the control of protein levels in eukaryotic cells that targets for degradation proteins covalently linked to the polypeptide ubiquitin. For a protein to be recognized by the 26S proteasome, a chain of at least four ubiquitin monomers is needed, which is delivered to the substrate by an ATP-dependent enzymatic E1–E2–E3 conjugation cascade (reviewed in Sadanandom et al., 2012). E3 ubiquitin ligases are the most numerous and diverse of the three groups of enzymes, being responsible for substrate recognition and specificity. Substrate phosphorylation is one of the signals recognized by some types of E3 ubiquitin ligase complexes (reviewed in Deshaies, 1999).

The most studied *Arabidopsis thaliana* SR-related protein is SR45, a *bona fide* splicing factor (Ali et al., 2007) that plays an established role in ABA responses (Carvalho et al., 2010, 2016; Xing et al., 2015; Albaqami et al., 2019). Having been classified as a canonical SR protein for many years, SR45 is currently considered an SR-like protein (Barta et al., 2010) owing to its two RS domains that flank a single RNA recognition motif (Golovkin and Reddy, 1999). The only *SR45* loss-of-function mutant described to date, *sr45-1*, exhibits a variety of developmental phenotypes, including reduced plant size, late and bushy inflorescences, and delayed root growth, as well as abnormal leaf and flower morphology (Ali et al., 2007). Moreover, *sr45-1* mutant seedlings are hypersensitive to ABA and glucose (Carvalho et al., 2010, 2016) as well as high salinity (Albaqami et al., 2019). Seven different splice variants of the *A. thaliana SR45* gene have been annotated, but only two have been characterized, *SR45.1* and *SR45.2*, which, despite exhibiting very similar expression patterns, fulfill different functions. Although both variants are able to rescue the mutant's glucose hypersensitivity (Carvalho et al., 2010), *SR45.2* rescues the root growth defect, whereas *SR45.1* rescues the flower (Zhang and Mount, 2009), salt (Albaqami et al., 2019), and (partially) ABA (Xing et al., 2015) phenotypes.

Interestingly, the 4262 RNAs reported by Xing et al. (2015) to bind SR45 include transcripts encoding 30% of all ABA signaling genes (Hauser et al., 2011). Furthermore, in addition to interacting with other splicing factors, including U1-70K (Golovkin and Reddy, 1999), U2AF (Day et al., 2012), three different U5 snRNP components, and several SR proteins (Golovkin and Reddy, 1999; Tanabe et al., 2009; Zhang et al., 2014), SR45 has been found to interact with two proteins involved in ABA responses: SKIP (SNW/SKI-INTERACTING PROTEIN) (Wang et al., 2012), a putative transcription factor conferring plant salt tolerance (Feng et al., 2015), and SUA (SUPPRESSOR OF ABI3-5) (Mukhtar et al., 2011), which controls alternative splicing of *ABA-INSENSITIVE 3* (*ABI3*) (Sugliani et al., 2010).

Several reports of phosphorylation at specific SR45 residues in different plant tissues and stress conditions have been published (De La Fuente Van Bentem et al., 2006, 2008; Umezawa et al., 2013; Wang et al., 2013; Zhang et al., 2014), with an early study showing that a LAMMER-type protein kinase, AFC2, can interact with and phosphorylate SR45 *in vitro* (Golovkin and Reddy, 1999). Moreover, Zhang et al. (2014) reported the relevance of phosphorylation of a single SR45 amino acid residue, T218, for both the regulation of flower development and the alternative splicing of a direct mRNA target. On the other hand, a phosphoproteomics study found evidence for ABA-induced dephosphorylation of SR45 at a different residue, T264 (Wang et al., 2013). Given that SR45 transcript and splicing levels are reportedly unchanged by ABA treatment (Palusa et al., 2007; Cruz et al., 2014), these data strongly suggest that SR45 is regulated by ABA at the posttranslational level.

How SR45 is posttranslationally regulated by ABA and related stresses remains largely unknown. Here we report that the *A. thaliana* SR45 protein accumulates and is dephosphorylated at several residues in response to ABA. We find that ABA-mediated dephosphorylation of the protein reduces its ubiquitination and targeting for proteasomal degradation, thus leading to SR45 stabilization under ABA conditions. Our results also demonstrate that the T264 residue of SR45 is sufficient to influence phosphorylation-dependent proteasomal degradation of the protein and thereby its function as a negative regulator of the ABA pathway, allowing some degree of plant growth and development under stress.

RESULTS

Overexpression of the SR45 protein causes plant ABA hyposensitivity

We previously showed that loss of function of the *Arabidopsis SR45* gene leads to enhanced sensitivity to the ABA hormone at the cotyledon greening stage (Carvalho et al., 2010), with Xing et al. (2015) later reporting that overexpression of the *SR45.1* splice variant partially rescues this ABA greening inhibition phenotype. Given that the *SR45* gene produces at least two splice isoforms with distinct functions (Zhang and Mount, 2009; Albaqami et al., 2019), we decided to investigate the effect of expressing the genomic *SR45* fragment on the ABA response of transgenic seedlings during early development. To this end, we cloned the gene's genomic fragment upstream of the EGFP sequence driven by either the endogenous *SR45* (pSR45:gSR45–eGFP) or the strong constitutive *UBQ10* (pUBQ10::gSR45–eGFP) promoter (Supplemental Figure 1). These two constructs were independently transformed into *sr45-1* mutant plants (Ali et al.,

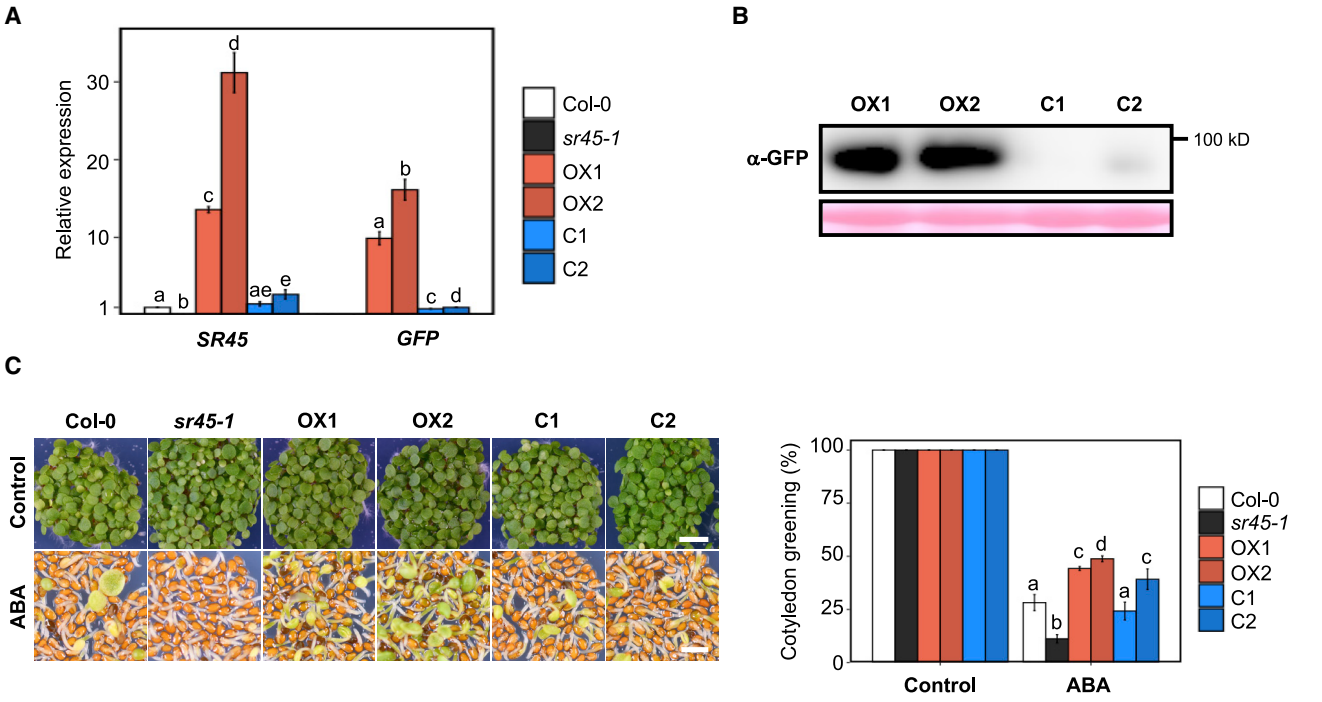

Figure 1. Effect of *SR45* overexpression on ABA signaling during cotyledon development.

(A) qRT-PCR analysis of *SR45–GFP* transcript levels in pUBQ10::SR45–GFP/*sr45-1* (OX1 and OX2) and pSR45::SR45–GFP/*sr45-1* (C1 and C2) transgenic seedlings, as well as in Col-0 wild-type and *sr45-1* mutant seedlings grown for 7 days under control conditions, using *PEX4* as a reference gene and primers annealing to either the *SR45* or the *GFP* sequence (see Supplemental Figure 1). Transcript levels of either the Col-0 (*SR45* primers) or the C2 transgenic line (*GFP* primers) were set to 1. Results represent means ± SE ($n = 3$), and different letters indicate statistically significant differences between genotypes for each set of primers ($P < 0.05$; Student's *t*-test).

(B) Protein gel blot analysis using α-GFP antibodies of the SR45–GFP fusion protein in 7-day-old seedlings of overexpression (OX1 and OX2) and complementation (C1 and C2) transgenic lines grown under control conditions. A total of 30 ng of protein was loaded per sample, and Ponceau staining is shown as a loading control. Results are representative of at least three independent experiments.

(C) Representative images and quantification of cotyledon greening in 7-day-old seedlings of the Col-0 wild type, the *sr45-1* mutant, the OX1 and OX2 overexpression lines, and the C1 and C2 complementation lines grown under control conditions or in the presence of 0.5 μM ABA (means ± SE, $n = 3$). Different letters indicate statistically significant differences between genotypes under each condition ($P < 0.05$; Student's *t*-test). Scale bars, 2.5 mm (control) or 1 mm (ABA).

2007), and two complementation (C1 and C2) and two overexpression (OX1 and OX2) transgenic lines were isolated for the pSR45::gSR45–eGFP and pUBQ10::gSR45–eGFP constructs, respectively.

As seen in Figure 1A, qRT-PCR analysis using primers specific for the *SR45* gene (see Supplemental Figure 1) revealed that the OX1 and OX2 lines express about 15- and 30-fold higher transcript levels than the Col-0 wild type, respectively, whereas in the C2 line, expression is enhanced by only ∼2.5 fold, and C1 expresses levels similar to the wild type. As expected, transcript levels were barely detectable in the *sr45-1* knockout mutant. Similar results were obtained when primers specific for the *GFP* coding sequence were used (see Supplemental Figure 1) and the expression levels of the transgene were normalized to those of the C2 complementation line (Figure 1A). Western blot analysis using anti-GFP antibodies showed that the relative differences in *SR45–GFP* transcript among the transgenic lines were matched at the protein level, as both overexpression lines showed highly elevated amounts of SR45–GFP compared with the complementation lines, with C2 exhibiting slightly higher levels of the fusion protein compared with C1 (Figure 1B).

Phenotypic characterization of the transgenic lines revealed no defects in cotyledon development under control conditions and full rescue of the ABA hypersensitivity of the *sr45-1* mutant (Figure 1C). Moreover, all plant lines expressing significantly enhanced *SR45* mRNA levels (OX1, OX2, and C2) displayed reduced sensitivity to exogenous ABA. Notably, OX2 was the transgenic line that displayed stronger ABA hyposensitivity, correlating with higher expression of the *SR45–GFP* transgene. Our results show that the function of SR45 as a negative regulator of ABA signaling during early seedling development is dependent on SR45 protein levels.

ABA enhances SR45 protein levels

Previous work indicates that the expression levels and splicing pattern of the *SR45* gene are unchanged by ABA (Palusa et al., 2007; Cruz et al., 2014), but it remains unknown whether SR45 protein levels are regulated by the phytohormone. To investigate this possibility, we treated seedlings from a transgenic complementation line with 2 μM ABA and followed SR45 protein levels for 3 h by western blotting. Results revealed an evident accumulation of the SR45–GFP fusion protein over time in the ABA-treated samples, with the highest levels detected after

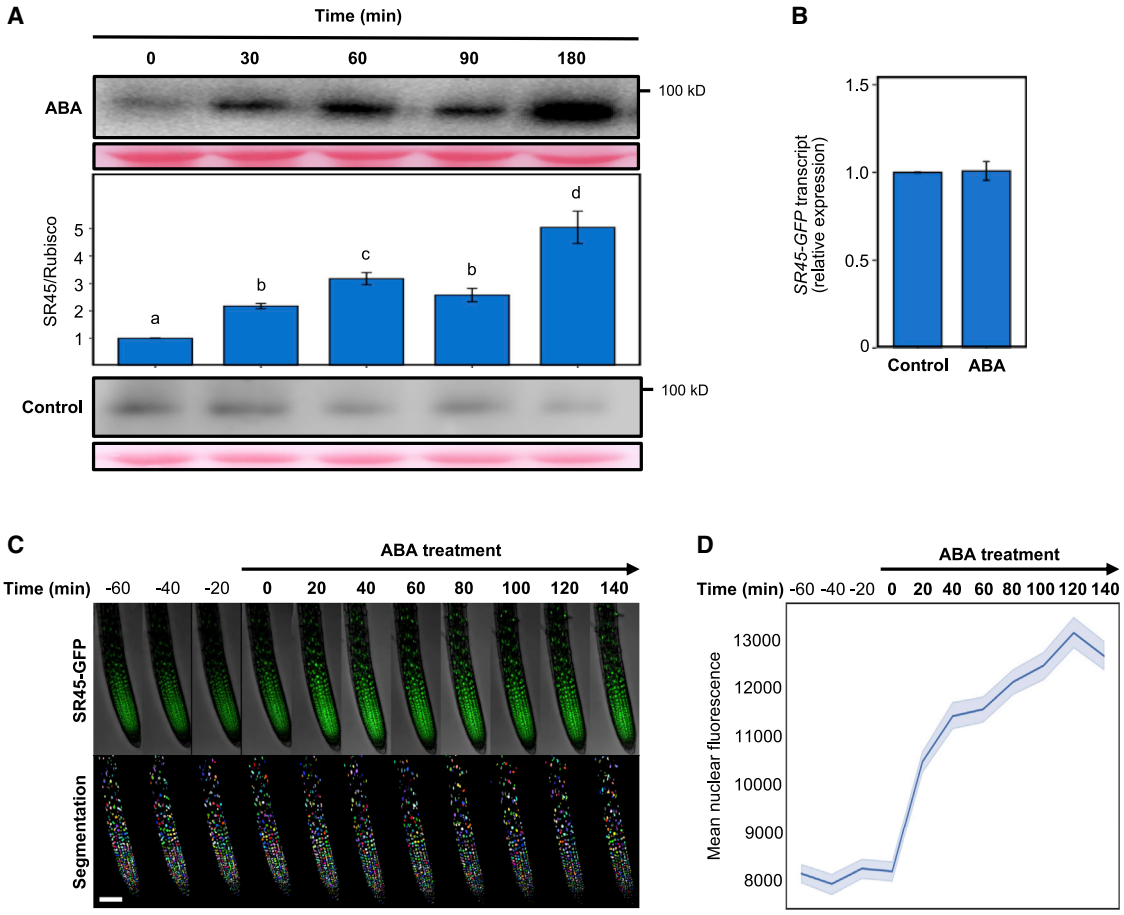

Figure 2. Effect of ABA on SR45 protein levels.

(A) Protein gel blot analysis using α-GFP antibodies of the SR45–GFP fusion protein in 7-day-old seedlings of the C2 complementation transgenic line treated for 0, 30, 60, 90, or 180 min with 2 μM ABA. Control samples were treated with the equivalent volume of the solvent of the ABA solution (ethanol). A total of 40 ng of protein was loaded per sample. Bands were quantified and relative protein levels determined using the Ponceau loading control as a reference, with control conditions set to 1. Results represent means ± SE ($n = 3$), and different letters indicate statistically significant differences between treatments ($P < 0.05$; Student's *t*-test).

(B) qRT-PCR analysis of SR45–GFP transcript levels in 2-day-old seedlings of the C2 complementation line (SR45–GFP/*sr45-1*) treated for 180 min with 1 μM ABA, using PEX4 as a reference gene and primers annealing to the GFP sequence (see Supplemental Figure 1). Control samples (set to 1) were treated with the equivalent volume of the solvent of the ABA solution (ethanol). Results represent means ± SE ($n = 3$), with no statistically significant differences found between treatments ($P > 0.05$; Student's *t*-test).

(C) Sum Z projection images (top) and segmentation (bottom) of fast SR45–GFP accumulation in the primary root of 4-day-old seedlings of the C2 complementation transgenic line treated with 10 μM ABA observed by confocal microscopy. Scale bar, 100 μm.

(D) Quantification of the nuclear intensity of the segmentation shown in **(C)**. Line indicates mean values, with shaded region indicating the 95% confidence interval.

180 min, whereas control samples harvested at the same time points showed no increase in SR45 protein levels (Figure 2A). Although endogenous *SR45* transcript levels are not regulated by ABA (Palusa et al., 2007; Cruz et al., 2014), we confirmed that our transgene was also not transcriptionally affected by ABA. As seen in Figure 2B, qRT-PCR analysis of the *SR45–GFP* transcript in SR45–GFP/*sr45-1* seedlings revealed no changes in expression levels upon ABA treatment.

A similar trend of SR45–GFP accumulation was observed in transgenic seedlings treated with ABA when the fluorescence intensity was measured in primary roots by confocal microscopy. Figure 2C and 2D shows that addition of 10 μM ABA to the sample buffer increased the mean SR45–GFP fluorescence intensity per segmented nucleus by approximately 50% in 150 min, unequivocally demonstrating that the amount of SR45 protein is upregulated by ABA.

ABA dephosphorylates SR45 and enhances its levels in a SnRK2-dependent manner

In a phosphoproteomics study by Wang et al. (2013), the phosphorylation levels of SR45 were reported to decrease in response to ABA treatment. To verify whether SR45 is dephosphorylated by ABA under our conditions, we treated seedlings from a complementation line with 2 μM ABA for 3 h and compared the phosphorylation status of the SR45–GFP fusion protein with that from seedlings subjected to a mock

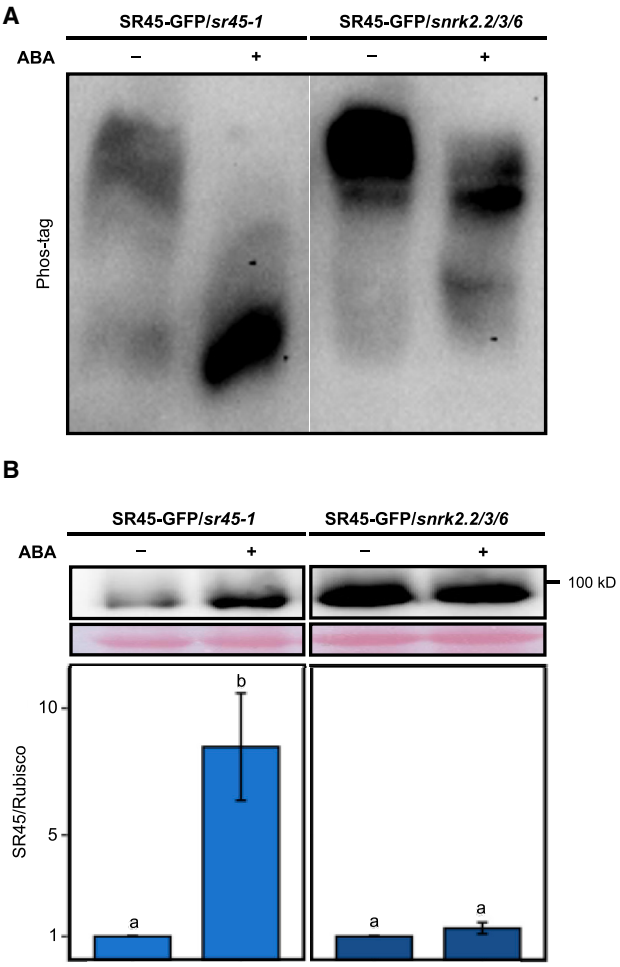

Figure 3. Effect of ABA on phosphorylation and amounts of the SR45 protein and dependence on SnRK2 function.

Phos-tag **(A)** and protein **(B)** gel blot analyses using α-GFP antibodies of the SR45–GFP fusion protein in 7-day-old seedlings of the C2 complementation line (SR45–GFP/*sr45-1*) and a transgenic line expressing the pSR45:gSR45–GFP construct in the *snrk2.2/3/6* mutant background (SR45–GFP/*snrk2.2/3/6*) treated for 180 min with 2 μM ABA. Control samples were treated with the equivalent volume of the solvent of the ABA solution (ethanol), and a total of 40 ng of protein was loaded per sample. In **(A)**, results are representative of at least three independent experiments. In **(B)**, bands were quantified and relative protein levels determined using the Ponceau loading control as a reference, with results representing means ± SE ($n = 4$), control conditions set to 1, and different letters indicating a statistically significant difference between treatments for each genotype ($P < 0.05$; Student's *t*-test). In both **(A)** and **(B)**, all samples were run in the same gel, but images were cropped to show the relevant genotypes alongside one another.

treatment. As evident from the Phos-tag gel in Figure 3A, SR45 is markedly dephosphorylated in response to ABA. To test whether dephosphorylation of SR45 is dependent on a functional ABA-signaling pathway, we next analyzed the phosphorylation levels of SR45 upon ABA treatment of transgenic plants expressing the pSR45::gSR45–eGFP construct in the *snrk2.2/3/6* triple mutant background. The SR45 dephosphorylation induced by ABA was severely impaired by loss of SnRK2 function, indicating that the switch in the protein's phosphorylation status depends on ABA signaling (Figure 3A). These Phos-tag analyses revealed the presence of several protein isoforms, whereas single bands had been detected in SDS–PAGE blots, thus indicating that SR45 can be phosphorylated at multiple amino acid residues. Moreover, control and ABA samples treated with λ phosphatase both displayed a band pattern similar to that induced by ABA exposure, demonstrating that the detected size shifts reflect differential phosphorylation (Supplemental Figure 2). Interestingly, we observed a clear SnRK2-dependent accumulation of the least phosphorylated form of SR45 in response to ABA, with two different phosphoisoforms accumulating in the ABA-treated *snrk2.2/3/6* line (Figure 3A).

Importantly, when SR45 protein levels were analyzed in the same samples by western blotting, the SR45 protein accumulation observed upon ABA treatment (see also Figure 2A) was abolished in the *snrk2.2/3/6* mutant background (Figure 3B), indicating that the ABA-induced increase in SR45 levels is fully dependent on ABA signaling downstream of SnRK2s and suggesting a putative link between dephosphorylation and accumulation of the SR45 protein. As in the complementation line (see also Figure 2B), qRT-PCR analysis of *SR45–GFP* transcript levels in SR45–GFP/*snrk2.2/3/6* seedlings revealed no changes upon ABA treatment (Supplemental Figure 3).

ABA stabilizes SR45 by reducing protein ubiquitination and proteasomal degradation

Having established that SR45 is regulated by ABA at the post-translational level, we hypothesized that the different amounts of SR45 protein observed under control and ABA conditions were due to differences in protein stability. To test this hypothesis, we treated seedlings with the potent proteasome inhibitor MG132 before exposure to ABA and determination of SR45–GFP protein levels by western blotting (Figure 4A). Notably, pretreatment with MG132 resulted in a significant increase in SR45 levels only in the absence of ABA, suppressing the difference in SR45 content between the control and ABA conditions (Figure 4A). This result indicates increased targeting of SR45 for proteasomal degradation under control conditions, strongly suggesting that ABA-dependent SR45 protein accumulation is due to increased stability of the SR45 protein under ABA conditions.

To verify that the differences in SR45 stability correlate with different ubiquitination levels of the protein, we immunoprecipitated SR45–GFP from protein extracts of seedlings treated with ABA and checked for the presence of ubiquitin conjugates (Figure 4B). As expected, for the same amount of immunoprecipitated protein loaded in the SDS–PAGE gel, more immunoprecipitated SR45–GFP was retrieved in ABA-treated samples compared with the control, but greater accumulation of ubiquitin was detected in control than in ABA pull-downs. Quantification of the ubiquitin signal and normalization to the amounts of immunoprecipitated SR45–GFP showed that the ubiquitination levels of the immunoprecipitated SR45–GFP were reduced by more than half under ABA conditions (Figure 4B). Immunoprecipitation of control 35S::GFP transgenic seedlings showed residual ubiquitin conjugates bound to GFP alone (Supplemental Figure 4).

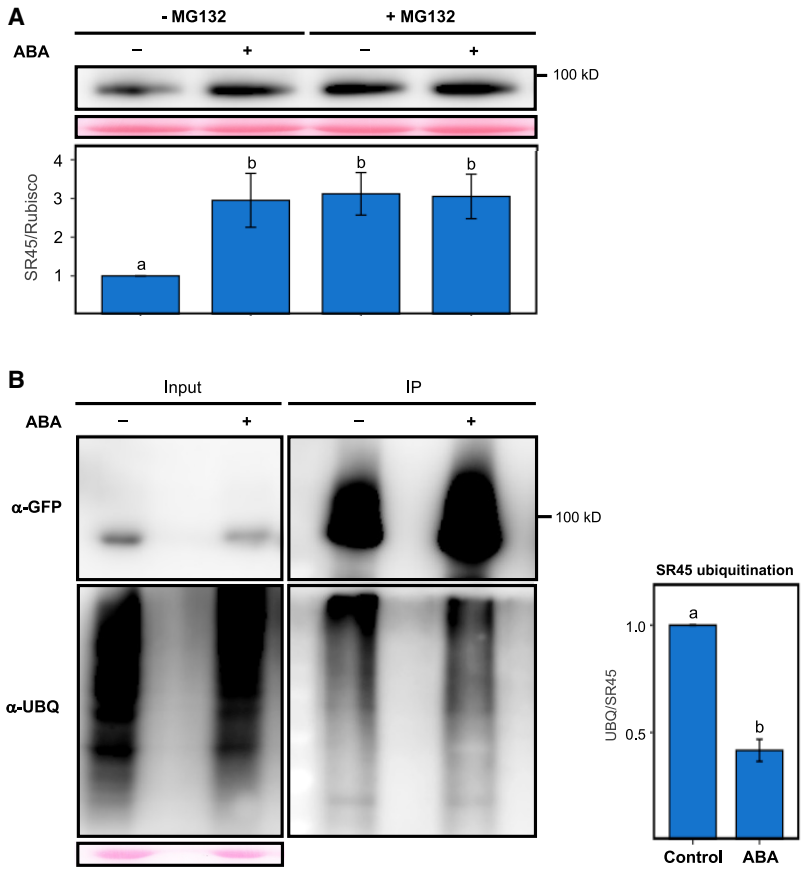

Figure 4. Effect of ABA on SR45 protein stability and ubiquitination.

(A) Protein gel blot analysis, using α-GFP antibodies, of the SR45–GFP fusion protein in 7-day-old seedlings of the C2 complementation line pretreated with MG132 and subjected to a 180-min treatment with 2 μM ABA. Control samples (−MG132 or −ABA) were treated with the equivalent volume of the solvent of the MG132 or ABA solution (DMSO or ethanol, respectively). A total of 40 ng of protein was loaded per sample. Bands were quantified and relative protein levels determined using the Ponceau loading control as a reference, with control conditions set to 1. Results represent means ± SE ($n = 4$), and different letters indicate statistically significant differences between treatments ($P < 0.05$; Student's t-test).

(B) Protein gel blot analysis of the SR45–GFP fusion protein immunoprecipitated from extracts of 7-day-old seedlings of the C2 complementation line treated for 180 min with 2 μM ABA using α-GFP (immunoprecipitation; IP) or α-UBQ11 (coIP) antibodies. Control samples were treated with the equivalent volume of the solvent of the ABA solution (ethanol). Ponceau staining is shown as a loading control for the input fraction. Signals were quantified and the UBQ/SR45–GFP ratio determined, with control conditions set to 1. Results represent means ± SE ($n = 3$), and different letters indicate statistically significant differences between treatments ($P < 0.05$; Student's t-test).

Together, these results show a higher degree of both SR45 ubiquitination and SR45 degradation by the ubiquitin–proteasome system under control conditions, with the protein being less ubiquitinated and more stable upon exposure to ABA.

Phosphorylation of the T264 residue controls SR45 protein ubiquitination and degradation

Given that phosphorylation-dependent protein ubiquitination and degradation is a known mechanism to rapidly control protein levels in both animal and plant systems (reviewed in Filipčík et al., 2017; Vu et al., 2018; Bhaskara et al., 2019), we next asked whether SR45 stability is dependent on the phosphorylation status of the protein. To address this question, we generated transgenic *Arabidopsis* lines expressing the pUBQ10::gSR45–eGFP construct mutated at a threonine (T) phosphoresidue reported by Wang et al. (2013). We changed this T264 residue to either alanine (A), an amino acid that cannot be phosphorylated (phosphomutant lines), or aspartic acid (D), which is structurally similar to a phosphorylated threonine and thus mimics constitutive phosphorylation (phosphomimetic lines).

To investigate whether SR45 phosphorylation at the T264 residue affects ubiquitination of the protein, we immunoprecipitated SR45–GFP from protein extracts of overexpression (OX1), phosphomutant (PMut1), and phosphomimetic (PMim1) transgenic seedlings grown under control conditions and checked for the presence of ubiquitin in the immunoprecipitates (Figure 5A). Quantification of the respective signals and calculation of the ubiquitin/SR45 ratio showed much higher ubiquitination levels in the pull-downs from the phosphomimetic line compared with the overexpression and phosphomutant lines. SR45–GFP immunoprecipitated from the latter line, in which T264 is never phosphorylated, showed the lowest degree of ubiquitination (Figure 5A). These results indicated that phosphorylation of the T264 residue promotes SR45 ubiquitination.

To verify that T264 phosphorylation also results in rapid destabilization of SR45, we next followed degradation of the protein through time. As observed in Figure 5B, SR45 decayed to about 60% of its initial levels in 15 min in the control overexpression line, but the protein was more rapidly degraded in the phosphomimetic line, falling to nearly 20% in the same time frame. By contrast, SR45 was markedly more stable in phosphomutant extracts, beginning to decay only after 30 min and falling to only about 50% of its initial level after an hour. Addition of the MG132 inhibitor to the protein extracts showed that the observed decay of the SR45 protein in all plant lines is proteasome dependent (Figure 5C). We thus concluded that T264 phosphorylation controls SR45 protein degradation via the ubiquitin–proteasome system; dephosphorylation of the protein at this residue results in reduced levels of ubiquitination and therefore enhanced protein stability.

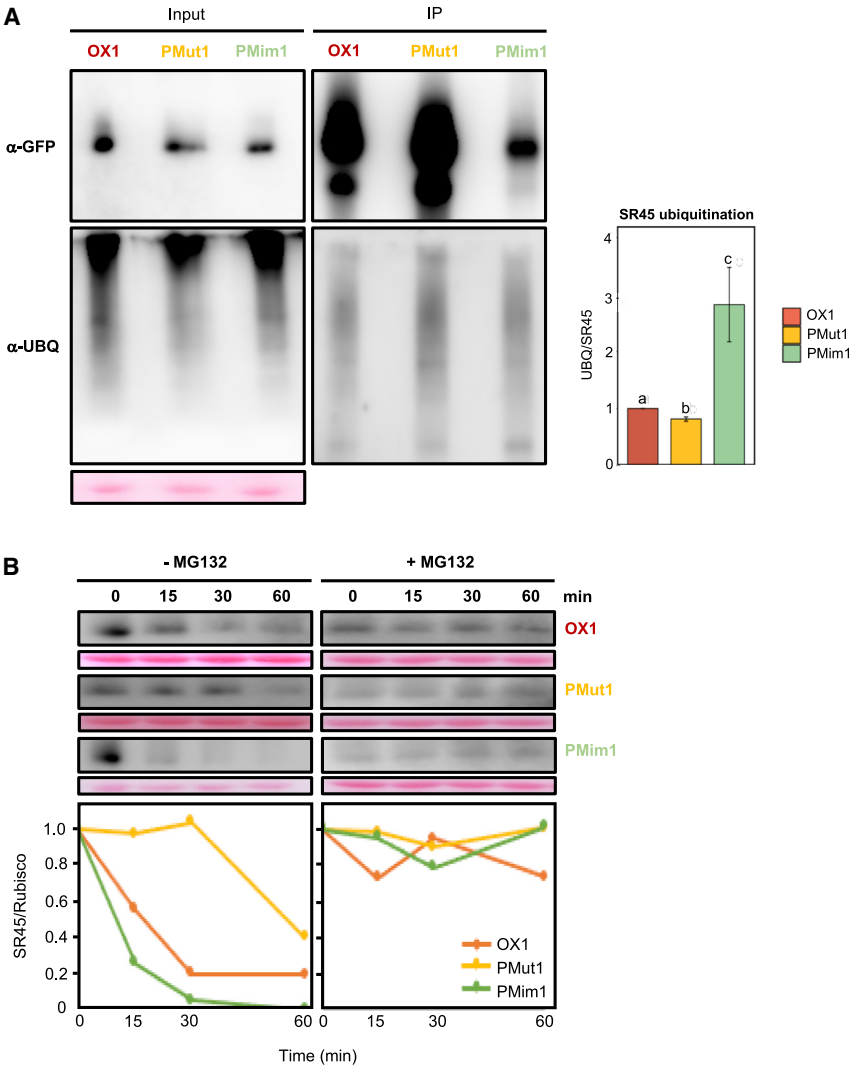

Figure 5. Effect of T264 phosphorylation on SR45 ubiquitination and degradation.

(A) Protein gel blot analysis of the SR45–GFP fusion protein immunoprecipitated from extracts of 7-day-old seedlings of the OX1 overexpression (pUBQ10:SR45–GFP/*sr45-1*), PMut1 phosphomutant (pUBQ10:SR45–GFP_T264A/*sr45-1*), and PMim1 phosphomimetic (pUBQ10:SR45–GFP_T264D/*sr45-1*) transgenic lines grown under control conditions using α-GFP (immunoprecipitation; IP) or α-UBQ11 (coIP) antibodies. Ponceau staining is shown as a loading control for the input fraction. Signals were quantified and the UBQ/SR45–GFP ratio determined, with control conditions set to 1. Results represent means ± SE (n = 3), and different letters indicate statistically significant differences between genotypes ($P < 0.05$; Student's t-test).

(B) Protein gel blot analysis, using α-GFP antibodies, of the SR45–GFP fusion protein in 7-day-old seedlings of the OX1 overexpression, PMut1 phosphomutant, and PMim1 phosphomimetic transgenic lines supplemented or not with MG132 and left at room temperature for 0, 15, 30, or 60 min. Control samples (−MG132) were treated with the equivalent volume of the solvent of the MG132 solution (DMSO), and a total of 20 ng of protein was loaded per sample. Bands were quantified and relative protein levels determined using the Ponceau loading control as a reference, with time 0 set to 1. Results are representative of at least three independent experiments.

Phosphorylation of the T264 residue controls ABA-induced SR45 protein accumulation and plant ABA sensitivity

Finally, we analyzed the effect of SR45 phosphorylation at the T264 residue on ABA responses. We first verified that the T264 residue is in fact differentially phosphorylated upon ABA exposure. As evident from the Phos-tag gel presented in Supplemental Figure 5, the unmutated OX1 overexpression line displayed clear accumulation of a less phosphorylated isoform under ABA conditions, but no isoform shift between control and ABA conditions was detected in either the PMut1 phosphomutant or the PMim1 phosphomimetic line, clearly showing that the T264 residue is differentially phosphorylated by ABA.

Next, to test ABA-driven SR45 protein accumulation, we treated seedlings from the OX1, PMut1, and PMim1 transgenic lines with 2 μM ABA and assessed SR45–GFP levels after 3 h by western blotting. As shown in Figure 6A, the accumulation of SR45–GFP under ABA conditions observed in the C2 complementation line (see Figures 2 and 3B) was reproduced in OX1, an overexpression line in which the transgene is driven by a different promoter, reinforcing the posttranslational regulation of SR45 by ABA. By contrast, ABA-induced SR45 protein accumulation was abolished in both the transgenic line in which SR45 cannot undergo phosphorylation at T264 (PMut1) and the line in which SR45 constitutively mimics phosphorylation at this residue (PMim1). We actually observed a slight decrease in SR45–GFP protein levels upon ABA treatment in the phosphomutant and phosphomimetic lines (Figure 6A), consistent with reduced transcript levels (Supplemental Figure 6), possibly due to ABA downregulation of *UBQ10* promoter activity. This transcriptional downregulation of transgene expression by ABA was also observed in an independent set of phosphotransgenic lines: OX2, PMut2, and PMim2 (Supplemental Figure 7A). An increase in SR45 protein levels in response to ABA treatment was again observed only in the overexpression line (Supplemental Figure 7B). These results demonstrate that a switch in phosphorylation status is required for SR45 protein accumulation in response to ABA exposure, supporting the notion that the ABA-induced increase inSR45 levels depends on dephosphorylation of the protein by the hormone.

Having gained molecular insight into the effects of the T264 mutation on SR45, we then asked whether it would have an impact on the plant's physiological response to ABA and affect sensitivity to the hormone during cotyledon greening. Figure 6B shows that phenotypic characterization of the transgenic OX1, PMut1, and PMim1 lines under control conditions revealed no differences in cotyledon development. However, whereas the OX1 and Pmut1 lines displayed similar reductions in cotyledon

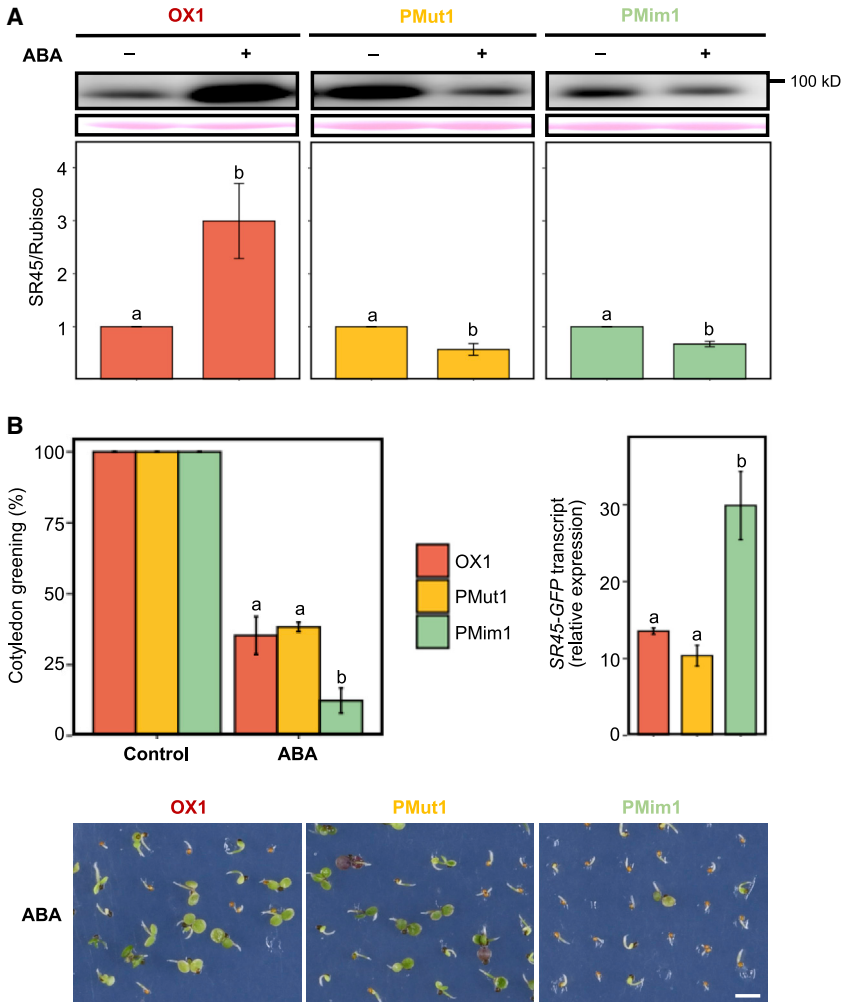

Figure 6. Effect of T264 phosphorylation on ABA-dependent SR45 protein accumulation and cotyledon development.

(A) Protein gel blot analysis, using α-GFP antibodies, of the SR45–GFP fusion protein in 7-day-old seedlings of the OX1 overexpression (pUBQ10:SR45–GFP/*sr45-1*), PMut1 phosphomutant (pUBQ10:SR45–GFP_T264A/*sr45-1*), and PMim1 phosphomimetic (pUBQ10:SR45–GFP_T264D/*sr45-1*) transgenic lines treated for 180 min with 2 μM ABA. Control samples were treated with the equivalent volume of the solvent of the ABA solution (ethanol), and a total of 20 ng of protein was loaded per sample. Bands were quantified and relative protein levels determined using the Ponceau loading control as a reference, with results representing means ± SE ($n = 3$), control conditions set to 1, and different letters indicating statistically significant differences between treatments for each genotype ($P < 0.05$; Student's *t*-test). All samples were run in the same gel, but images were cropped to show the relevant genotypes alongside one another.

(B) Cotyledon greening percentages of 7-day-old seedlings of the OX1 overexpression, PMut1 phosphomutant, and PMim1 phosphomimetic transgenic lines grown under control conditions or in the presence of 0.5 μM ABA, with representative images of ABA conditions (scale bar, 0.2 cm), and qRT-PCR analysis of *SR45–GFP* transcript levels in the same seedlings (control conditions), using *PEX4* as a reference gene and primers annealing to the *GFP* sequence (see Supplemental Figure 1). Results represent means ± SE ($n = 3$), and different letters indicate statistically significant differences between genotypes ($P < 0.05$; Student's *t*-test).

greening when grown in ABA, the PMim1 phosphomimetic seedlings showed a higher sensitivity to ABA, despite the fact that this particular line expressed about twice as much SR45–GFP mRNA (Figure 6B and Supplemental Figure 8). A similar result was obtained when independent transgenic lines (OX2, PMut2, and PMim2) were isolated and analyzed, with the PMim2 phosphomimetic line being clearly the most sensitive to ABA (Supplemental Figure 9). In this case, OX2 was less sensitive to ABA compared with PMut2, most likely because of markedly higher *SR45–GFP* transcript levels in the former transgenic line (Supplemental Figures 8 and 9). In conclusion, the enhanced ABA sensitivity of SR45 phosphomimetic transgenic lines in which the T264 residue mimics constitutive phosphorylation indicates that SR45 depends on dephosphorylation to enhance its levels and exert its role as a negative regulator of ABA responses during early plant development.

DISCUSSION

One important function of the ABA phytohormone is to arrest early seedling growth in challenging environments in order to mount a stress response and ensure survival. How plants negatively regulate the ABA pathway to maintain some degree of growth and development under stress is largely unclear. Here we show that overexpression of the *Arabidopsis SR45* gene causes reduced plant sensitivity to ABA during early development. Whereas Carvalho et al. (2010) observed complete rescue of the partially ABA-dependent *sr45-1* glucose phenotype upon overexpression of either the *SR45.1* or the *SR45.2* splice variant, Xing et al. (2015) found that overexpression of the *SR45.1* splice variant partially reverts *sr45-1* ABA hypersensitivity during early seedling development. Neither study identified an ABA-hyposensitive phenotype upon *SR45* overexpression, perhaps because individual *SR45* splice variants were tested independently instead of the genomic fragment. Seven *SR45* transcripts are currently annotated, and at least *SR45.1* and *SR45.2* are known to fulfill different biological roles (Zhang and Mount, 2009; Albaqami et al., 2019), rendering it likely that a combination of SR45 splice forms is required for the protein's role as a negative regulator of the ABA pathway. Alternatively, the ability to reduce ABA sensitivity could arise from the use of different promoters to drive the *SR45* transgene. The genomic construct is driven by the *UBQ10* promoter in our overexpression lines, whereas previous work used *35S*, whose activity can vary in different organs and under abiotic stress (Kiselev et al., 2021). Nevertheless, we recently also found opposite ABA and ABA-related phenotypes for the loss-of-function mutant and *Arabidopsis* lines expressing the SCL30a SR protein under the control of the 35S promoter (Laloum et al., 2021).

SR proteins are established phosphoproteins, and several phosphorylation residues have been annotated for SR45. Moreover, a phosphoproteomics study listed SR45 as displaying reduced phosphorylation under ABA conditions (Wang et al., 2013). Consistent with these results, we found that upon ABA exposure, SR45 is dephosphorylated at several residues in a SnRK2-dependent manner, indicating that ABA signaling downstream of SnRK2 kinases either activates phosphatases that dephosphorylate SR45 or deactivates kinases that phosphorylate SR45 under control conditions. Interestingly, we detected ABA-induced accumulation of a specific SR45 phosphoisoform (Figure 3A) in the *snrk2.2/3/6* background, suggesting that this SR45 (de)phosphorylation event occurs either through ABA signaling upstream of SnRK2s or independently of these core ABA pathway components. SnRK2-independent ABA signaling, in which PP2C phosphatases dephosphorylate other kinases that activate different branches of ABA signaling, has previously been reported (Brandt et al., 2012). Our findings fit with the general model in which dephosphorylation negatively regulates ABA signaling (reviewed in Yang et al., 2017). In fact, several PP2C phosphatases are known to negatively regulate ABA signaling, and the corresponding loss-of-function mutants display ABA-hypersensitive phenotypes (Merlot et al., 2001; Yoshida et al., 2006; Nishimura et al., 2007), as observed for SR45.

Importantly, we found that the SR45 protein accumulates upon ABA treatment in a SnRK2-dependent manner and that the phosphorylation status of the protein controls this ABA-induced increase in SR45 levels. Indeed, using phosphomutant and phosphomimetic lines in which the SR45 protein is never phosphorylated or mimics constitutive phosphorylation at T264, a previously reported ABA-specific SR45 dephosphorylation residue (Wang et al., 2013), we showed that: (i) a switch in SR45 phosphorylation status is required for ABA induction of SR45 protein accumulation, (ii) dephosphorylation of the T264 residue upon ABA exposure results in reduced ubiquitination levels and lower proteasomal degradation rates of SR45, and (iii) SR45 phosphorylation at T264 enhances plant ABA sensitivity at the early seedling stage.

Our results demonstrate functional and physiological relevance for ABA-mediated posttranslational modification of an SR-related splicing factor that negatively regulates ABA responses during early plant development (Carvalho et al., 2010; Xing et al., 2015). We show that SR45 is phosphorylated under control conditions, with phosphorylation of a single residue being able to modulate the protein's ubiquitination levels and the amounts of SR45 that are targeted for degradation by the ubiquitin–proteasome system. Upon exposure to ABA, downstream signaling triggers SR45 dephosphorylation, thus reducing both the ubiquitination and the degradation rates of the protein. Consistent with ABA stabilization of the SR45 protein, we also demonstrate that the protein's role as a negative regulator of the ABA pathway is dependent on SR45 protein levels, pointing to ABA-induced SR45 accumulation as a mechanism of negative autoregulation of ABA signaling. Also in agreement with our model (Figure 7), SR45 phosphomimetic lines are more sensitive to ABA: when T264 dephosphorylation is prevented, SR45 is degraded at higher rates, resulting in lower amounts of SR45 protein and enhanced seedling sensitivity to ABA. Given that SR45 is dephosphorylated by ABA, both the overexpression and the phosphomutant lines display a decreased ABA response. Figure 7 illustrates the biological significance of our findings: when stress is perceived and ABA levels increase sharply, seedling growth is repressed but so is phosphodegradation of SR45; as the splicing factor gradually accumulates, ABA-mediated inhibition of seedling development is alleviated to allow a physiological trade-off between growth and stress tolerance.

In plants, protein phosphodegradation is crucial for regulation of the phytochrome interacting factor 5 (PIF5) and PIF3 transcription factors involved in light signaling (Al-Sady et al., 2006; Shen et al., 2007; Yue et al., 2016), but it has also been shown to directly regulate key ABA signaling components, including the *Arabidopsis* PYR/PYL receptors (Chen et al., 2018), DREB2A (DEHYDRATION-RESPONSIVE ELEMENT-BINDING PROTEIN 2A) (Mizoi et al., 2019), and RopGEF1 (GUANINE NUCLEOTIDE EXCHANGE FACTOR 1) (Li et al., 2016, 2018). Moreover, the RING-type E3 ligase KEG (KEEP ON GOING) regulates itself via ABA-dependent phosphodegradation, thereby stabilizing the ABI5 (ABA-INSENSITIVE 5) transcription factor, which is ubiquitinated by this E3 ligase (Liu and Stone, 2010). As for SR proteins, although their phosphorylation-dependent degradation has not yet been reported, a couple of studies in humans have looked into both phosphorylation and proteasomal degradation of these RNA-binding proteins. Breig and Baklouti (2013) found that mutating an AKT-signaling phosphorylation site has no effect on proteasomal degradation of the human SR protein SRSF5, whereas acetylation downregulates phosphorylation levels and promotes degradation of SRSF2, suggesting a link between acetylation and phosphorylation in regulating the levels of this SR protein (Edmond et al., 2011).

In line with our findings, UBQ3 (POLYUBIQUITIN 3) is a reported interactor of *Arabidopsis* SR45 (Kim et al., 2013). SR45 has also been reported to interact with the products of the At2g43770 and At1g10580 genes (Zhang et al., 2014), which are predicted to contain WD40 domains (Zhang et al., 2008). WD40 proteins function as potential substrate receptors of CUL4 E3 ubiquitin ligases (Lee et al., 2008), and it is interesting to note that two components of these E3 ligases are also reported to be negative regulators of ABA signaling (Lee et al., 2010). However, phosphorylated substrates are usually recognized by F-box proteins, which are part of the Skp1–Cullin–F-box complex, a different major type of E3 ubiquitin ligase (reviewed in Deshaies, 1999; Sadanandom et al., 2012). Further biochemical and genetic studies should enable identification of both the kinases or phosphatases and the E3 ligase complexes that regulate SR45 protein levels and unveil the precise molecular mechanisms that lead to SR45 dephosphorylation and accumulation in response to ABA.

METHODS

Plant materials

The *A. thaliana* Colombia ecotype (Col-0) was used as the wild type in all experiments. The *sr45-1* knockout homozygous line was originally isolated in the Duque lab (Carvalho et al., 2010). The *snrk2.2/3/6* triple mutant was kindly provided by P.L. Rodríguez (Universidad Politécnica de Valencia, Spain).

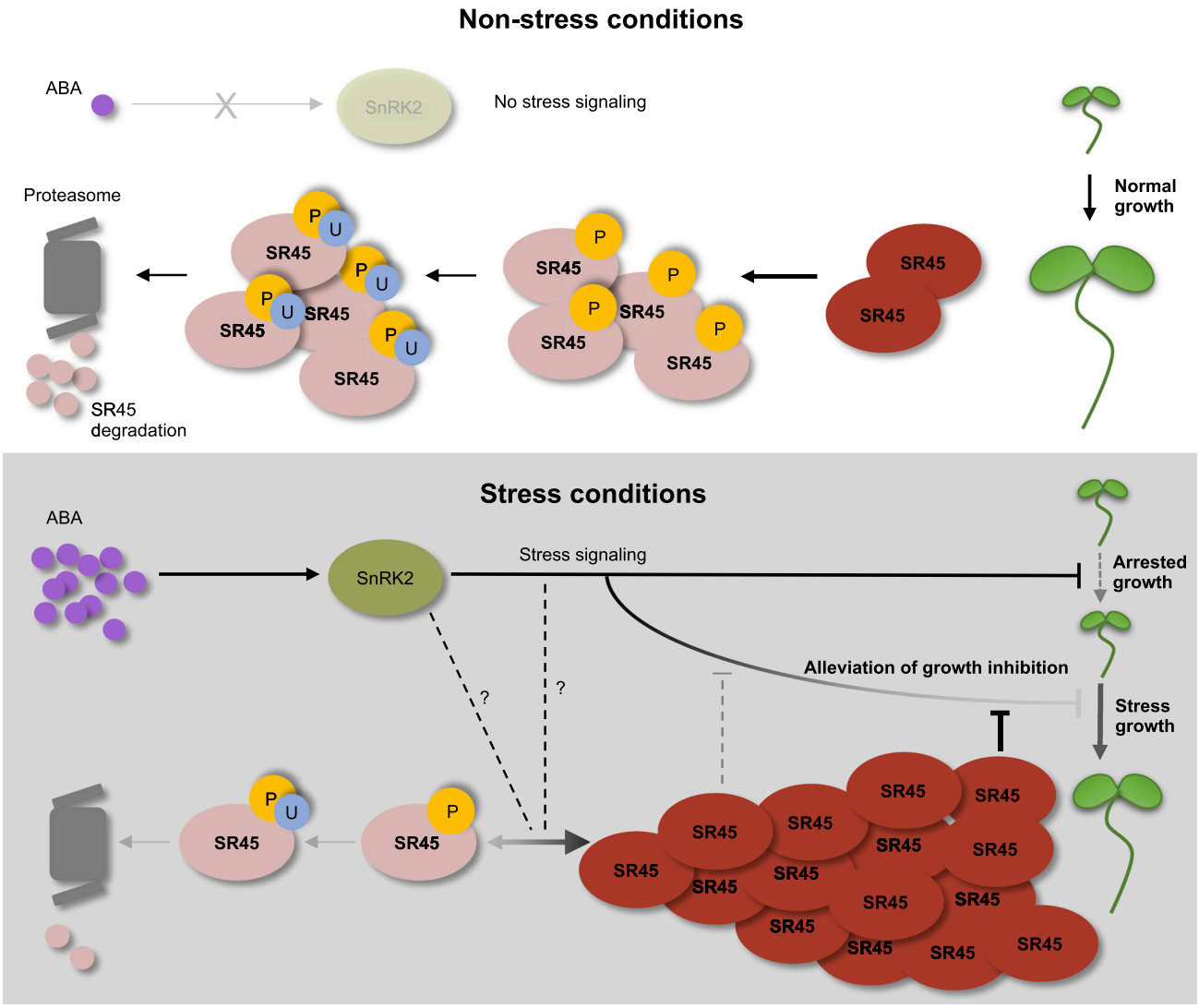

Figure 7. Model of ABA-mediated SR45 regulation of early seedling development.
Under non-stress conditions, basal ABA levels, which are insufficient to activate stress signaling, allow normal plant growth, with phosphorylation of SR45 triggering its ubiquitination and subsequent proteasomal degradation. In response to stress, ABA accumulates in the cell, activating SnRK2s and thus downstream signaling. This reduces SR45 phosphorylation levels via a yet unknown mechanism, leading to reduced ubiquitination and stabilization of the protein. Gradual accumulation of SR45 results in negative regulation of ABA signaling, alleviating its inhibition of early seedling development and allowing plant growth to some extent under stress conditions.

Generation of transgenic lines

To generate the pSR45::gSR45–eGFP constructs, a fragment including the *SR45* promoter and its genomic sequence was isolated by PCR using primers annealing 1252 bp upstream and 2756 bp downstream of the *SR45* start codon (Supplemental Table 1) and Col-0 DNA as a template. The *SR45* amplicon was subcloned into the pGEM-T Easy vector and incorporated into a GFP-tagged version of the binary pBA002 vector using the BspEI/PacI restriction sites. The construct was then used to transform the *Arabidopsis sr45-1* and *snrk2.2/3/6* mutants by the floral dip method (Clough and Bent, 1998) using *Agrobacterium tumefaciens* strain GV3101.

The full-length *SR45* fragment (excluding the stop codon) was amplified using primers with attB1/attB2 MultiSite Gateway sites (Supplemental Table 1). An entry clone was generated by introducing the amplicon into pDONR 221 (Invitrogen) by recombination. The entry clone *SR45* in pDONR 221, along with vectors with the ubiquitin-10 promoter (UBQ10) in pDONR P4-P1R (Invitrogen) and *eGFP* in pDONR P2R-P3 (Invitrogen), was recombined with the destination vector pHm43GW to generate the pUBQ10::gSR45–eGFP overexpression construct as described in Hartley et al. (2000). To generate SR45 variants carrying the T264A and T264D mutations, site-directed mutagenesis was performed using *Pfu* DNA polymerase on *SR45* in the pDONR 221 clone using different primer pairs (Supplemental Table 1). The resulting clones were further recombined with *UBQ10* in pDONR P4-P1R and *eGFP* in pDONR P2R-P3 in the pHm43GW destination vector as described above for the over-expression construct. Each construct was independently transformed into *sr45-1* mutant plants by agroinfiltration. All experiments with transgenic lines were conducted on isolated T3 homozygous lines.

Plant growth

For all phenotype assays, seeds were surface sterilized for 10 min with 50% (v/v) bleach and 0.02% (v/v) Tween X-100 under continuous shaking and then washed three times in sterile water. Approximately 100 seeds per genotype were plated in triplicate on half-strength MS medium (0.5× MS

basal salt mix, Duchefa Biochemie; 0.5 mM *myo*-inositol; 2.5 mM MES; and 0.8% agar, adjusted to pH 5.7) supplemented or not with 0.5 μM ABA (S-ABA, Duchefa Biochemie). The plates were wrapped in aluminum foil and stored at 4°C for 3 days. After stratification, the plates were transferred to a growth chamber under continuous light (100 μmol m^{-2} s^{-1}) at 22°C. The percentage of green seedlings was calculated relative to the total number of germinated seeds (displaying an emerged radicle) after 7 days. The average of the percentages was calculated per genotype, and statistical differences between genotypes were assessed using Student's *t*-test.

For protein extraction, seedlings were grown for 5 days in 0.5× MS agar medium under continuous light (100 μmol m^{-2} s^{-1}) at 22°C. The seedlings were then transferred to liquid 0.5× MS medium and grown with constant shaking for 48 h under the same growth conditions. At this stage, control (ethanol) or 2 μM ABA (S-ABA, Duchefa Biochemie; ethanol stock) treatment was applied for specific amounts of time (0, 30, 60, 90, or 180 min). To inhibit proteasomal degradation, 50 μM MG132 (Sigma, C2211; DMSO stock) or DMSO (control) was added 60 min prior to the onset of the ABA treatment. The plant material was harvested and frozen at −80°C for protein extraction.

To compare the RNA levels of all transgenic lines, plants were also grown for 5 days in 0.5× MS agar medium under continuous light and transferred to liquid 0.5× MS medium for 48 h with constant shaking. To test for transcriptional ABA regulation, 2-day-old seedlings were grown on a paper filter and placed on 0.5× MS agar medium plates under continuous light conditions. The seedlings were then transferred to 0.5× MS agar medium supplemented with 1 μM ABA or ethanol (control) and grown for 180 min before harvesting.

RNA extraction and qRT-PCR analyses

Total RNA was extracted from *Arabidopsis* seedlings using the innuPREP Plant RNA kit (Analytik Jena BioSolutions). All RNA samples were treated with DNase I (Promega), and cDNA was synthesized using SuperScript III reverse transcriptase (Invitrogen) and oligo$(dT)_{18}$ primers. qRT-PCR was performed using an ABI QuantStudio 384-well instrument (Applied Biosystems) and Luminaris Color HiGreen qPCR master mix High ROX (Thermo Scientific) with 2.5 μl of cDNA (diluted 1:20) per 10-μl reaction volume containing 300 nM of each specific primer (Supplemental Table 1). Cycle threshold values were adjusted for each gene in each biological replicate. Relative expression values were generated for the target gene using a log2 transformation, normalizing the gene cycle threshold values to the housekeeping control gene *PEX4* (*PEROXIN4*) as described in Vandesompele et al. (2002). The average value of the relative expression of each gene in all biological replicates was calculated per sample. Statistical differences between the average relative expression values of individual samples were inferred using Student's *t*-test.

Microscopy analyses

For confocal microscopy analysis, *sr45-1* seedlings expressing the pSR45:gSR45–eGFP construct were mounted on slides in a vacuum grease/coverslip reservoir as described in Rizza et al. (2019) in 0.25× MS. Seedlings were imaged for an hour of pretreatment, and then a buffer exchange to 0.25× MS + 10 μM ABA was performed and imaging was resumed. Confocal images were acquired on an upright Leica SP8 microscope using an HC PL APO CS2 20×/0.75 DRY objective. The emission laser and detection windows were as follows: GFP, 488 nm laser, 493–568 nm detection; gain, 200. A custom Fiji (Schneider et al., 2012; Rueden et al., 2017) plug in, "Simple_auto_segmentation.py," was developed using CLIJ2 (Haase et al., 2020) to perform segmentation and fluorescence quantification per nucleus. Source code and installation instructions are available at https://github.com/JimageJ/ImageJ-Tools. This plug in preprocesses images for segmentation with difference of Gaussian and top-hat filters followed by thresholding using Otsu's method. A watershed and connected-components analysis are used to split and identify objects in the threshold image. Any objects lost in watershed are added back in, and a non-zero dilation and multiplication is used to expand the object map into the original binary map to produce the final segmentation. The segmentation is then used to extract the 3D position, size, and intensity of every nucleus in the image Z stack, enabling changes in protein levels to be quantified at the cellular level.

Protein extraction, western blotting, and Phos-tag assays

Frozen 7-day-old *Arabidopsis* seedlings subjected to prior treatments were ground with a mortar and pestle under liquid nitrogen. Total protein was extracted in an extraction buffer containing 50 mM Tris-HCl, 150 mM NaCl, 1 mM EDTA, 0.5% Triton X-100 (Sigma-Aldrich), 1 tablet of Complete Protease Inhibitor Cocktail (Roche), and 1 tablet of PHOSSTOP (Roche). The extract was centrifuged at 18 000 *g* for 10 min at 4°C and the protein content of the supernatant determined using the Bradford method (Bio-Rad) in a spectrophotometer measuring the absorbance at 595 nm, followed by elution in Laemmli 2× buffer with 8% β-mercaptoethanol (95°C for 5 min). After the protein concentration in each sample was determined, equal amounts of protein were resolved on 8% SDS–polyacrylamide gels. The proteins were then transferred to PVDF membranes (Immobilon-P, Millipore) and blocked with 5% non-fat dry milk for 2 h. The membranes were probed overnight at 4°C with anti-GFP primary antibodies (Roche, 11814460001; 1:1000) and then with anti-mouse peroxidase-conjugated secondary antibodies (Jackson ImmunoResearch, 115-035-146; 1:4000) for 2 h at room temperature. All antibodies were diluted in TBS buffer (25 mM Tris-HCl [pH 7.4] and 137 mM NaCl) supplemented with 1% non-fat dry milk. After incubation with the antibodies, the membranes were washed with TBS containing 0.05% Tween 20 (Sigma-Aldrich) for 40 min. The peroxidase activity associated with the membrane was visualized by enhanced chemiluminescence. The intensity of the protein bands was quantified using ImageJ software, normalizing protein levels to that of the Rubisco large subunit visualized in membranes stained with 0.1% Ponceau S (Sigma-Aldrich) in 5% acetic acid. Statistical differences between the average protein levels of each sample were inferred using Student's *t*-test.

To separate the different SR45 phosphoisoforms under control and ABA conditions, Mn^{2+}-Phos-tag SDS–PAGE was performed. Equivalent amounts of total protein were loaded and resolved on a 6% acrylamide gel with 50 μM $MnCl_2$ and 25 μM Phos-tag (Wako Pure Chemical Industries). Each sample was supplemented with 1:10 $MnCl_2$ to minimize the "smiling" effect before the run. For phosphatase treatment, after protein extraction, each extract was supplemented 1:10 with λ phosphatase (λPPase, New England BioLabs) and 1:10 with $MnCl_2$ (10 mM solution) and further incubated for 30 min at 30°C. The gel was washed twice for 20 min with transfer buffer (25 mM Tris, 192 mM glycine, 0.1% SDS, and 20% ethanol) supplemented with 1 mM EDTA, followed by an additional wash with regular transfer buffer for 10 min. The proteins were wet-transferred to a PVDF membrane (Immobilon-P, Millipore) for 2.5 h at 100 V. The membrane was blocked and probed with antisera as described above.

SR45–GFP immunoprecipitation and protein degradation assay

Total protein was extracted from approximately 100 mg of 7-day-old *Arabidopsis* seedlings with 800 μl of the extraction buffer described above. The extract was centrifuged at 18 000 *g* for 10 min at 4°C and the supernatant incubated for 1 h at 4°C with continuous agitation with 100 μl of Sepharose beads (Sigma-Aldrich). The extract was then further centrifuged at 500 *g* for 2 min, and the input fraction was removed and eluted in Laemmli 2× buffer for 5 min at 95°C. After incubation with 20 μl of GFP-Trap agarose beads (ChromoTek) for 1.5 h, the beads were washed three times with cold extraction buffer for 10 min each, and the proteins were eluted from the beads in 30 μl of Laemmli 2× buffer for 5 min at 95°C. Finally, 15 μl of the immunoprecipitate and 20 μl of the input fraction were loaded on separate SDS–PAGE gels, with blotting performed as described above. For detection of UBQ conjugates, the membranes

were stripped for 15 min with Western BLoT Stripping Buffer (TaKaRa) following the manufacturer's instructions and reprobed with Ubiquitin11 (Agrisera AS08307; 1/10 000) and anti-rabbit peroxidase-conjugated secondary antibodies (Amersham Pharmacia; 1/10 000). The intensity of the protein bands was quantified using ImageJ software. Statistical differences between the average ratios of each sample were inferred using Student's *t*-test.

The degradation rate of the SR45 protein was assessed in protein extracts from 7-day-old seedlings grown under control conditions supplemented with 50 μM MG132 or DMSO (control) and left to degrade at room temperature for 0, 15, 30, and 60 min. The protein extracts were loaded on an SDS–PAGE gel, and blotting was performed as described above.

SUPPLEMENTAL INFORMATION

Supplemental information is available at *Plant Communications Online*.

FUNDING

This work was funded by the Fundação para a Ciência e a Tecnologia (FCT) through grant PTDC/ASP-PLA/2550/2021 and a PhD fellowship PD/BD/128401/2017 awarded to R.A.-M. Funding from the research unit GREEN-it "Bioresources for Sustainability" (UIDB/04551/2020) is also acknowledged. A.M.J. and J.R. were funded by the Gatsby Charitable Foundation and BBSRC (BB/P018572/1).

AUTHOR CONTRIBUTIONS

R.A.-M., A.M.J., and P.D. designed the research; R.A.-M., D.S., and J.R. performed the experiments; and A.M.J. and P.D. supervised the work. R.A.-M. and P.D. wrote the manuscript and prepared the figures and tables. All authors contributed to the interpretation of results, critically reviewed the manuscript, and approved its final version.

ACKNOWLEDGMENTS

We thank P.L. Rodríguez for the *snrk2.2/3/6* triple mutant, L. Margalha for expert biochemistry advice, and V. Nunes for excellent plant care at the Instituto Gulbenkian de Ciência (IGC) Plant Facility, as well as E. Baena-González, I. Abreu, and A. Confraria for helpful discussions. No conflict of interest is declared.

Received: February 27, 2022
Revised: August 12, 2022
Accepted: November 18, 2022
Published: November 23, 2022

REFERENCES

Al-Sady, B., Ni, W., Kircher, S., Schäfer, E., and Quail, P.H. (2006). Photoactivated phytochrome induces rapid PIF3 phosphorylation prior to proteasome-mediated degradation. Mol. Cell **23**:439–446.

Albaqami, M., Laluk, K., and Reddy, A.S.N. (2019). The Arabidopsis splicing regulator SR45 confers salt tolerance in a splice isoform-dependent manner. Plant Mol. Biol. **100**:379–390.

Ali, G.S., Palusa, S.G., Golovkin, M., Prasad, J., Manley, J.L., and Reddy, A.S.N. (2007). Regulation of plant developmental processes by a novel splicing factor. PLoS One **2**:e471.

Barta, A., Kalyna, M., and Reddy. (2010). Implementing a Rational and Consistent Nomenclature for Serine / Arginine-Rich Protein Splicing Factors (SR Proteins) in Plants **22**:2926–2929.

Bhaskara, G.B., Wong, M.M., and Verslues, P.E. (2019). The flip side of phospho-signalling: regulation of protein dephosphorylation and the protein phosphatase 2Cs. Plant Cell Environ. **42**:2913–2930.

Brandt, B., Brodsky, D.E., Xue, S., Negi, J., Iba, K., Kangasjärvi, J., Ghassemian, M., Stephan, A.B., Hu, H., and Schroeder, J.I. (2012). Reconstitution of abscisic acid activation of SLAC1 anion channel by CPK6 and OST1 kinases and branched ABI1 PP2C phosphatase action. Proc. Natl. Acad. Sci. USA **109**:10593–10598.

Breig, O., and Baklouti, F. (2013). Proteasome-mediated proteolysis of SRSF5 splicing factor intriguingly Co-occurs with SRSF5 mRNA upregulation during late erythroid differentiation. PLoS One **8**:e59137.

Carvalho, R.F., Carvalho, S.D., and Duque, P. (2010). The plant-specific SR45 protein negatively regulates glucose and ABA signaling during early seedling development in arabidopsis. Plant Physiol. **154**:772–783.

Carvalho, R.F., Szakonyi, D., Simpson, C.G., Barbosa, I.C.R., Brown, J.W.S., Baena-González, E., and Duque, P. (2016). The arabidopsis SR45 splicing factor, a negative regulator of sugar signaling, modulates SNF1-related protein kinase 1 stability. Plant Cell **28**:1910–1925.

Chen, T., Cui, P., Chen, H., Ali, S., Zhang, S., and Xiong, L. (2013). A KH-domain RNA-binding protein interacts with FIERY2/CTD phosphatase-like 1 and splicing factors and is important for pre-mRNA splicing in arabidopsis. PLoS Genet. **9**. e1003875.

Chen, H.H., Qu, L., Xu, Z.H., Zhu, J.K., and Xue, H.W. (2018). EL1-like casein kinases suppress ABA signaling and responses by phosphorylating and destabilizing the ABA receptors PYR/PYLs in arabidopsis. Mol. Plant **11**:706–719.

Clough, S.J., and Bent, A.F. (1998). Floral dip: a simplified method for Agrobacterium-mediated transformation of Arabidopsis thaliana. Plant J. **16**:735–743.

Cruz, T., Carvalho, R., Richardson, D., and Duque, P. (2014). Abscisic acid (ABA) regulation of arabidopsis SR protein gene expression. Int. J. Mol. Sci. **15**:17541–17564.

Day, I.S., Golovkin, M., Palusa, S.G., Link, A., Ali, G.S., Thomas, J., Richardson, D.N., and Reddy, A.S.N. (2012). Interactions of SR45, an SR-like protein, with spliceosomal proteins and an intronic sequence: insights into regulated splicing. Plant J. **71**:936–947.

De La Fuente Van Bentem, S., Anrather, D., Roitinger, E., Djamei, A., Hufnagl, T., Barta, A., Csaszar, E., Dohnal, I., Lecourieux, D., and Hirt, H. (2006). Phosphoproteomics reveals extensive in vivo phosphorylation of Arabidopsis proteins involved in RNA metabolism. Nucleic Acids Res. **34**:3267–3278.

De La Fuente Van Bentem, S., Anrather, D., Dohnal, I., Roitinger, E., Csaszar, E., Joore, J., Buijnink, J., Carreri, A., Forzani, C., Lorkovic, Z.J., et al. (2008). Site-specific phosphorylation profiling of arabidopsis proteins by mass spectrometry and peptide chip analysis. J. Proteome Res. **7**:2458–2470.

Deshaies, R.J. (1999). SCF and Cullin/Ring H2-based ubiquitin ligases. Annu. Rev. Cell Dev. Biol. **15**:435–467.

Duque, P. (2011). A role for SR proteins in plant stress responses. Plant Signal. Behav. **6**:49–54.

Edmond, V., Moysan, E., Khochbin, S., Matthias, P., Brambilla, C., Brambilla, E., Gazzeri, S., and Eymin, B. (2011). Acetylation and phosphorylation of SRSF2 control cell fate decision in response to cisplatin. EMBO J. **30**:510–523.

Fàbregas, N., Yoshida, T., and Fernie, A.R. (2020). Role of Raf-like kinases in SnRK2 activation and osmotic stress response in plants. Nat. Commun. **11**:6184.

Feng, Y., Chen, M., and Manley, J.L. (2008). Phosphorylation switches the general splicing repressor SRp38 to a sequence-specific activator. Nat. Struct. Mol. Biol. **15**:1040–1048.

Feng, J., Li, J., Gao, Z., Lu, Y., Yu, J., Zheng, Q., Yan, S., Zhang, W., He, H., Ma, L., and Zhu, Z. (2015). SKIP confers osmotic tolerance during salt stress by controlling alternative gene splicing in arabidopsis. Mol. Plant **8**:1038–1052.

Filipčík, P., Curry, J.R., and Mace, P.D. (2017). When worlds collide—mechanisms at the interface between phosphorylation and ubiquitination. J. Mol. Biol. **429**:1097–1113.

Finkelstein, R. (2013). Abscisic acid synthesis and response. Arabidopsis Book **11**:e0166.

Golovkin, M., and Reddy, A.S. (1999). An SC35-like protein and a novel serine/arginine-rich protein interact with Arabidopsis U1-70K protein. J. Biol. Chem. **274**:36428–36438.

Haase, R., Royer, L.A., Steinbach, P., Schmidt, D., Dibrov, A., Schmidt, U., Weigert, M., Maghelli, N., Tomancak, P., Jug, F., and Myers, E.W. (2020). CLIJ: GPU-accelerated image processing for everyone. Nat. Methods **17**:5–6.

Hartley, J.L., Temple, G.F., and Brasch, M.A. (2000). DNA cloning using in vitro site-specific recombination. Genome Res. **10**:1788–1795.

Hauser, F., Waadt, R., and Schroeder, J.I. (2011). Evolution of abscisic acid synthesis and signaling mechanisms. Curr. Biol. **21**:R346–R355.

Huang, Y., Yario, T.A., and Steitz, J.A. (2004). A molecular link between SR protein dephosphorylation and mRNA export. Proc. Natl. Acad. Sci. USA **101**:9666–9670.

Kim, D.Y., Scalf, M., Smith, L.M., and Vierstra, R.D. (2013). Advanced proteomic analyses yield a deep catalog of ubiquitylation targets in Arabidopsis. Plant Cell **25**:1523–1540.

Kiselev, K.V., Aleynova, O.A., Ogneva, Z.V., Suprun, A.R., and Dubrovina, A.S. (2021). 35S promoter-driven transgenes are variably expressed in different organs of Arabidopsis thaliana and in response to abiotic stress. Mol. Biol. Rep. **48**:2235–2241.

Laloum, T., Carvalho, S.D., Martín, G., Richardson, D.N., Cruz, T.M.D., Carvalho, R.F., Stecca, K.L., Kinney, A.J., Zeidler, M., Barbosa, I.C.R., et al. (2021). The plant-specific SCL30a SR protein regulates ABA-dependent seed traits and salt stress tolerance during germination. Preprint at bioRxiv. https://doi.org/10.1101/2021.10.13.464208.

Lee, J.H., Terzaghi, W., Gusmaroli, G., Charron, J.B.F., Yoon, H.J., Chen, H., He, Y.J., Xiong, Y., and Deng, X.W. (2008). Characterization of Arabidopsis and rice DWD proteins and their roles as substrate receptors for CUL4-RING E3 ubiquitin ligases. Plant Cell **20**:152–167.

Lee, J.H., Yoon, H.J., Terzaghi, W., Martinez, C., Dai, M., Li, J., Byun, M.O., and Deng, X.W. (2010). DWA1 and DWA2, two Arabidopsis DWD protein components of CUL4-based E3 ligases, act together as negative regulators in ABA signal transduction. Plant Cell **22**:1716–1732.

Li, Z., Waadt, R., and Schroeder, J.I. (2016). Release of GTP exchange factor mediated down-regulation of abscisic acid signal transduction through ABA-induced rapid degradation of RopGEFs. PLoS Biol. **14**. e1002461.

Li, Z., Takahashi, Y., Scavo, A., Brandt, B., Nguyen, D., Rieu, P., and Schroeder, J.I. (2018). Abscisic acid-induced degradation of Arabidopsis guanine nucleotide exchange factor requires calcium-dependent protein kinases. Proc. Natl. Acad. Sci. USA **115**:E4522–E4531.

Liu, H., and Stone, S.L. (2010). Abscisic acid increases Arabidopsis ABI5 transcription factor levels by promoting KEG E3 ligase self-ubiquitination and proteasomal degradation. Plant Cell **22**:2630–2641.

Merlot, S., Gosti, F., Guerrier, D., Vavasseur, A., and Giraudat, J. (2001). The ABI1 and ABI2 protein phosphatases 2C act in a negative feedback regulatory loop of the abscisic acid signalling pathway. Plant J. **25**:295–303.

Mizoi, J., Kanazawa, N., Kidokoro, S., Takahashi, F., Qin, F., Morimoto, K., Shinozaki, K., and Yamaguchi-Shinozaki, K. (2019). Heat-induced inhibition of phosphorylation of the stress-protective transcription factor DREB2A promotes thermotolerance of Arabidopsis thaliana. J. Biol. Chem. **294**:902–917.

Mukhtar, M.S., Carvunis, A.R., Dreze, M., Epple, P., Steinbrenner, J., Moore, J., Tasan, M., Galli, M., Hao, T., Nishimura, M.T., et al. (2011). Independently evolved virulence effectors converge onto hubs in a plant immune system network. Science **333**:596–601.

Nishimura, N., Yoshida, T., Kitahata, N., Asami, T., Shinozaki, K., and Hirayama, T. (2007). ABA-Hypersensitive Germination1 encodes a protein phosphatase 2C, an essential component of abscisic acid signaling in Arabidopsis seed. Plant J. **50**:935–949.

Palusa, S.G., Ali, G.S., and Reddy, A.S.N. (2007). Alternative splicing of pre-mRNAs of Arabidopsis serine/arginine-rich proteins: regulation by hormones and stresses. Plant J. **49**:1091–1107.

Rizza, A., Walia, A., Tang, B., and Jones, A.M. (2019). Visualizing cellular gibberellin levels using the nlsGPS1 förster resonance energy transfer (FRET) biosensor. J. Vis. Exp. e58739.

Rueden, C.T., Schindelin, J., Hiner, M.C., DeZonia, B.E., Walter, A.E., Arena, E.T., and Eliceiri, K.W. (2017). ImageJ2: ImageJ for the next generation of scientific image data. BMC Bioinf. **18**:529.

Sadanandom, A., Bailey, M., Ewan, R., Lee, J., and Nelis, S. (2012). The ubiquitin-proteasome system: central modifier of plant signalling. New Phytol. **196**:13–28.

Sah, S.K., Reddy, K.R., and Li, J. (2016). Abscisic acid and abiotic stress tolerance in crop plants. Front. Plant Sci. **7**:571.

Sanford, J.R., Ellis, J.D., Cazalla, D., and Cáceres, J.F. (2005). Reversible phosphorylation differentially affects nuclear and cytoplasmic functions of splicing factor 2/alternative splicing factor. Proc. Natl. Acad. Sci. USA **102**:15042–15047.

Schneider, C.A., Rasband, W.S., and Eliceiri, K.W. (2012). NIH Image to ImageJ: 25 years of image analysis. Nat. Methods **9**:671–675.

Shen, Y., Khanna, R., Carle, C.M., and Quail, P.H. (2007). Phytochrome induces rapid PIF5 phosphorylation and degradation in response to red-light activation. Plant Physiol. **145**:1043–1051.

Shi, Y., and Manley, J.L. (2007). A complex signaling pathway regulates SRp38 phosphorylation and pre-mRNA splicing in response to heat shock. Mol. Cell **28**:79–90.

Sugliani, M., Brambilla, V., Clerkx, E.J.M., Koornneef, M., and Soppe, W.J.J. (2010). The conserved splicing factor SUA controls alternative splicing of the developmental regulator ABI3 in arabidopsis. Plant Cell **22**:1936–1946.

Tanabe, N., Kimura, A., Yoshimura, K., and Shigeoka, S. (2009). Plant-specific SR-related protein atSR45a interacts with spliceosomal proteins in plant nucleus. Plant Mol. Biol. **70**:241–252.

Umezawa, T., Sugiyama, N., Takahashi, F., Anderson, J.C., Ishihama, Y., Peck, S.C., and Shinozaki, K. (2013). Genetics and phosphoproteomics reveal a protein phosphorylation network in the abscisic acid signaling pathway in Arabidopsis thaliana. Sci. Signal. **6**.

Vandesompele, J., De Preter, K., Pattyn, F., Poppe, B., Van Roy, N., De Paepe, A., and Speleman, F. (2002). Accurate normalization of real-time quantitative RT-PCR data by geometric averaging of multiple internal control genes. Genome Biol. **3**. research0034.

Vu, L.D., Gevaert, K., and De Smet, I. (2018). Protein Language: post-translational modifications talking to each other. Trends Plant Sci. **23**:1068–1080.

Wang, X., Wu, F., Xie, Q., Wang, H., Wang, Y., Yue, Y., Gahura, O., Ma, S., Liu, L., Cao, Y., et al. (2012). SKIP is a component of the spliceosome linking alternative splicing and the circadian clock in Arabidopsis. Plant Cell **24**:3278–3295.

Wang, P., Xue, L., Batelli, G., Lee, S., Hou, Y.-J., Van Oosten, M.J., Zhang, H., Tao, W.A., and Zhu, J.-K. (2013). Quantitative phosphoproteomics identifies SnRK2 protein kinase substrates and reveals the effectors of abscisic acid action. Proc Natl Acad Sci USA **110**:11205–11210.

Xing, D., Wang, Y., Hamilton, M., Ben-Hur, A., and Reddy, A.S.N. (2015). Transcriptome-wide identification of RNA targets of

arabidopsis SERINE/ARGININE-RICH45 uncovers the unexpected roles of this RNA binding protein in RNA processingopen. Plant Cell **27**:3294–3308.

Yang, W., Zhang, W., and Wang, X. (2017). Post-translational control of ABA signalling: the roles of protein phosphorylation and ubiquitination. Plant Biotechnol. J. **15**:4–14.

Yoshida, T., Nishimura, N., Kitahata, N., Kuromori, T., Ito, T., Asami, T., Shinozaki, K., and Hirayama, T. (2006). ABA-hypersensitive germination3 encodes a protein phosphatase 2C (AtPP2CA) that strongly regulates abscisic acid signaling during germination among Arabidopsis protein phosphatase 2Cs. Plant Physiol. **140**:115–126.

Yue, J., Qin, Q., Meng, S., Jing, H., Gou, X., Li, J., and Hou, S. (2016). TOPP4 regulates the stability of PHYTOCHROME INTERACTING FACTOR5 during photomorphogenesis in Arabidopsis. Plant Physiol. **170**:1381–1397.

Zhang, X.N., and Mount, S.M. (2009). Two alternatively spliced isoforms of the Arabidopsis SR45 protein have distinct roles during normal plant development. Plant Physiol. **150**:1450–1458.

Zhang, Y., Feng, S., Chen, F., Chen, H., Wang, J., McCall, C., Xiong, Y., and Deng, X.W. (2008). Arabidopsis DDB1-CUL4 associated factor1 forms a nuclear E3 ubiquitin ligase with DDB1 and CUL4 that is involved in multiple plant developmental processes. Plant Cell **20**:1437–1455.

Zhang, X.N., Mo, C., Garrett, W.M., and Cooper, B. (2014). Phosphothreonine 218 is required for the function of SR45.1 in regulating flower petal development in arabidopsis. Plant Signal. Behav. **9**. e29134.